Biotechnology Notes 6 (2025) 133–142

Contents lists available at ScienceDirect

Biotechnology Notes

journal homepage: www.keaipublishing.com/en/journals/biotechnology-notes/

Research Article

# Development of a low-cost microfluidic chip for hyaluronidase-free oocyte denudation in mammals

Ashraf Hisham Dessouky [a,b,*], Haitham El-Hussieny [a], Taymour Mohammed El-Sherry [c], Victor Parque [d], Ahmed M.R. Fath El-Bab [a]

[a] Department of Mechatronics and Robotics Engineering, Egypt-Japan University of Science and Technology (E-JUST), Alexandria, 21934, Alexandria, Egypt
[b] Mechanical Engineering Department, Helwan University, Cairo, 11792, Cairo, Egypt
[c] Department of Theriogenology, Veterinary Hospital, Faculty of Veterinary Medicine Assiut University, Assiut, Assiut, Egypt
[d] Graduate School of Advanced Science and Engineering, Hiroshima University, HigashiHiroshima, 739-8527, Hiroshima, Japan

ARTICLE INFO

*Keywords:*
Microfluidics
Oocyte denudation
$CO_2$ laser
In vitro fertilization

ABSTRACT

Infertility in mammals is one of the most intricate medical issues requiring non-traditional interventions. In Vitro Fertilization (IVF) is one of the modern medical technologies currently used to treat infertility. However, current IVF procedures are inaccessible and unaffordable to the majority due to the high cost, the complexity of the procedure, and the reliance on highly qualified operators. For successful IVF, oocyte denudation, the process of removing cumulus cells from oocytes, is often performed. Here, microfluidics offers the potential to enhance denudation procedures and to minimize operator variability. In this paper, we propose the configuration of a microfluidic chip for oocyte denudation whose structure hybridizes inner jagged surfaces and expansion units. The jagged surface units have the role of removing the cumulus cells surrounding the oocyte by using the wall shear stress principle, and the (rounded) expansion units have the role of rotating the cumulus cells for further deployment in subsequent jagged surfaces. The proposed device can be manufactured at a low cost (<1 USD)) by the engraving of $CO_2$ laser machine on PMMA material, and is able to circumvent the use of enzymatic components such as hyaluronidase. Experiments using computational simulations and manufactured microfluidic chips evaluated distinct geometry configurations of the jagged surfaces and identified the suitable flow rates for maximal shear stress and denudation performance. Manufactured samples of the proposed microfluidic devices have shown the denudation performance of 96.7 % and yield rate of 90 % at a constant flow rate of 1 ml/min.

## 1. Introduction

Infertility is a disease denoting the inability to conceive a child after 12 months (or more) of consistent, unprotected sexual activity.[1] Worldwide, the incidence of infertility among couples in reproductive age ranges from 12.6 % to 17.5 % in the Americas, Western Pacific, Africa, and Europe[2]; and, according to the World Health Organization (WHO), 1 in 6 people show traits of infertility.[3] Assisted reproductive technology (ART), such as in vitro fertilization (IVF) and intracytoplasmic sperm injection (ICSI),[4] are well-known technologies targeting infertility treatment. And in vitro oocyte maturation is an appealing approach for human ART, offering advantages such as reduced cost and risks (e.g. ovarian hyperstimulation syndrome).[5] However, despite the advances in ART-based treatment of infertility, the current procedures induce in high cost and social stigma and have a limited accessibility.[6] Furthermore, since the current ART procedures lack standardization frameworks and depend on highly skilled individuals, operator-to-operator performance differences are often observed in the literature.[7]

Having relevant applications in the field of biomedical research[8] and ART,[9] microfluidics is a trending technology aiming at manipulating fluids and particles in microchannels.[10] For instance, microfluidic fertilization exposed pig and mouse oocytes in narrow channels to medium flow and semen.[11–13] In the context of IVF, sperm sorting and oocyte denudation are key to realize successful IVF. In the ovary, the oocyte is surrounded by cumulus cells (specialized granulosa cells),

Peer review under the responsibility of Editorial Board of Biotechnology Notes.
* Corresponding author. Department of Mechatronics and Robotics Engineering, Egypt-Japan University of Science and Technology (E-JUST), Alexandria, 21934, Alexandria, Egypt.
*E-mail addresses:* ashraf.dessouky@ejust.edu.eg, ashrafhisham41@h-eng.helwan.edu.eg (A.H. Dessouky).

https://doi.org/10.1016/j.biotno.2025.03.001
Received 4 January 2025; Received in revised form 21 February 2025; Accepted 10 March 2025
Available online 12 March 2025
2665-9069/© 2025 The Authors. Publishing services by Elsevier B.V. on behalf of KeAi Communications Co. Ltd. This is an open access article under the CC BY-NC-ND license (http://creativecommons.org/licenses/by-nc-nd/4.0/).

**Table 1**
Comparison of the proposed approach with the relevant works for oocyte denudation.

| Feature | Zeringue et al.[17] (2001) | Weng et al.[18] (2018) | Zhai et al.[19] (2022) | Mokhtare et al.[20] (2022) | This Work |
|---|---|---|---|---|---|
| Type | Microfluidic | Microfluidic | Robot System | Ultrasonic Device | **Microfluidic** |
| Material | PDMS | PDMS | Pipette | $LiNbO_3$ substrate and Interdigitated transducers | **PMMA** |
| Fabrication Method | Micromolding | Soft Lithography | NA | Surface acoustic waves with PDMS microchannel | **Direct Engraving** $CO_2$ Laser Machine |
| Cost | Very High (200–1000 USD) | Very High (200–1000 USD) | High | High | **Low** (<1 USD) |
| Hyaluronidase Usage | Not mentioned | Yes | No | No | **No** |
| System Structure | Multi-Process | Multi-Channel (100 constriction-expansion units) | Robotic system with a manipulator | Four interdigitated transducers (IDT) and fabrication of PDMS | **Simple Structure** (3 jagged units and two expansion units) |
| Denudation Efficiency | NA | 93.7 % | 95.0 ± 0.8 % | NA | **96.7 %** |

forming an overall structure known as the cumulus-oocyte-complex (COC), which develop cytoplasmic projections that cross the zona pellucida and form gap junctions with the Oolemma.[14] In vivo, the cumulus cell mass is removed from the oocyte upon fertilization through natural process.[15] In IVF clinics, cumulus cells are often removed from the oocytes to facilitate fertilization using the enzymatic action of hyaluronidase and (mechanical) pipetting. Often, denudation facilitates the fertilization process because of enhancing the injection of the sperm into the oocyte.[16]

Zeringue et al.[17,21] created a microfluidic device to mechanically remove the cumulus cells from single bovine zygotes. The cumulus cell mass was partially removed and reoriented. After that, the cumulus-zygote complex traveled through a marginally smaller and narrow channel, and then two suction ports, being narrower than the complex, were used to remove the remaining corona cells from the oocyte. The device allowed one zygote at a time, whereas the cumulus-zygote complex was positioned and moved by manual method that involved switching multiple fluid flows.

Recently, Weng et al.[18] developed a microfluidic device to remove the cumulus cells from mouse oocytes. Hyaluronidase-treated COCs, at either the germinal-vesicle or metaphase II stage, passed through a series of jagged-surface microchannels. The cumulus cells were stripped off by the inner wall of the constriction channel when processing COCs through at least 100 repeats of expansion (500 μm long and 500 μm wide) and constriction (640 μm long and 90 μm wide) units at a flow rate of 1 ml/min.

Hyaluronidase is often used in reproductive techniques to detach cumulus cells from the oocytes.[22,23] Hyaluronidase is an enzyme that hydrolyzes hyaluronan (hyaluronic acid or hyaluronate): a polysaccharide consisting of repeating disaccharide units of N-acetyl-D--glucosamine and D-glucuronic acid.[24] In the extracellular space of cumulus-oocyte complexes, hyaluronan is a highly hydrated and viscoelastic matrix.[25] Treatment with hyaluronidase causes the decomposition of the hyaluronan-based matrix surrounding COCs and disperses the cumulus cells from oocytes.[26,27] Treatment of human oocytes with hyaluronidases decreased oocyte survival, fertilization rates, and negatively impacts the developmental rates following ICSI.[28–30] In addition, the fertilization rate of the mouse oocyte decreased with hyaluronidase treatments. Also, oocytes treated with hyaluronidase for 5 min or longer had a reduced capacity to develop to the morula and blastocyst stage.[31]

Utilizing the relationship between oocyte quality and sedimentation rate, Iwasaki et al.[32] created a microfluidic device to separate high-quality bovine oocytes, thereby increasing the success rate of in vitro fertilization. The mechanical stress rises when the oocytes travel in the microchannels because of the physical contact between the cells and the inner wall of the channel. Luo et al.[33] studied the deformation of the mouse oocyte under shear flow as the oocytes traveled through constricted microfluidic channels at different sizes with various flow rates. Although shear stress is useful for oocyte denudation and helps to remove the cumulus cells, the shear stress is often controlled by flow rate manipulation and channel geometry adaptation.

Polymethyl Methacrylate (PMMA) material has been used to fabricate microfluidic chips in different bio-applications, such as Deoxyribonucleic acid (DNA), Polymerase Chain Reaction (PCR), and cell separation.[34–36] PMMA-based microfluidic chips for sperm sorting have been created using the rheotaxis technique.[37,38] Also, the direct engraving technique was used to fabricate different microfluidic chip materials using a laser beam in many bio-applications.[39–41] Micro biosensors have been developed using PMMA material.[42] In addition, the micromachining of PMMA using a $CO_2$ laser has been studied before.[43–47]

To realize a low-cost, hyaluronidase-free and efficient oocyte denudation approach, this paper capitalizes on microfluidics principles and PMMA material to propose a low-cost yet efficient oocyte denudation approach. In particular, our contributions are as follows:

- The configuration of a microfluidic chip for oocyte denudation whose structure hybridizes inner jagged surface and expansion units. Whereas the jagged surface units aims at removing the cumulus cells surrounding the oocyte by using the shear stress, the (rounded) expansion units facilitate the rotational motions for further deployment to subsequent jagged surfaces. Compared to the related approaches, the proposed microfluidic device can be manufactured at a low cost by the engraving of $CO_2$ laser machine on PMMA material, and is able to circumvent the use of enzymatic components such as hyaluronidase. Table 1 compares the proposed approach with the relevant works in oocyte denudation.
- The set of experiments using computational simulations and manufactured microfluidic chips evaluating (1) distinct configurations of the inclination angle of the jagged surfaces and flow rate actuation, and (2) the suitable flow rates for maximal shear stress. Manufactured samples of the proposed microfluidic devices has shown the denudation performance of 96.7 % and yield rate of 90 % at a constant flow rate of 1 ml/min.

The remaining of this paper is organized as follows: section 2 describes the materials and methods behind the proposed microfluidic chip, section 3 describes and discusses our simulation and experimental results, and section 4 concludes our paper.

## 2. Materials and methods

### 2.1. Oocyte preparation

The ovaries from a female slaughtered buffalo were extracted in Dachlout Abattoir, Dayrout, Assiut Governorate (Egypt). After washing and cleaning procedures at the Veterinary Medicine Department of Assiut University, oocytes were extracted into a Tissue Culture Medium

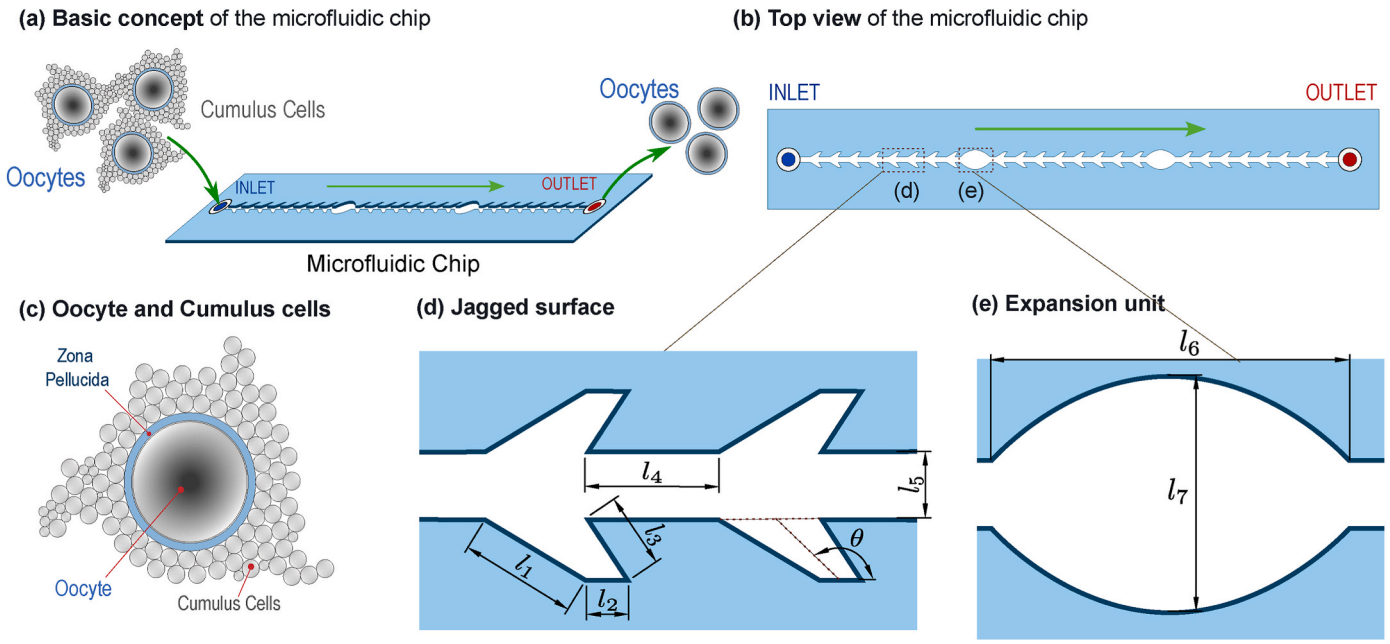


**Fig. 1.** Basic concept of the microfluidic chip for oocyte denudation.

199 (TCM 199) (BIO-CHEM, Belgium) for storage. For maturation process, the oocytes with Tissue Culture Medium 199 (TCM 199) were placed in tubes inside a $CO_2$ Incubator (N-BIOTEK Co, Korea) at 38 °C with 5 % $CO_2$ for 22–24 h.

### 2.2. Microfluidic structure

The structure of the proposed microfluidics chip consists of microchannels implementing inner jagged surface units and expansion units. The goal of using a microfluidic chip is to denudate the oocyte, i.e. separate the oocytes from the cumulus cells, as shown by Fig. 1. The jagged surface units enable to capitalize from enhanced fluid dynamics and wall shear stress that act on the COCs to remove the cumulus cells, whereas the (rounded) expansion units facilitate the rotational motions for further deployment to jagged surfaces. Overall, the chip has two expansion units and three jagged surface units. The oocytes with cumulus cells are injected from the inlet and allowed to go through the jagged surfaces and expansion units. Sharp turns are avoided to prevent oocyte trapping and to enhance yield rate. Relevant parameters include lengths $l_i (i \in [1, 7])$, inclination angle $\theta$ and number of jagged teeth, input flow rate, and number of expansion units.

### 2.3. Fabrication methodology

To fabricate the microfluidic chip, we used a $CO_2$ laser machine (VLS3.5, Universal Laser Systems, Kanagawa, Japan) with a 30-W laser tube and a laser lens (HPDFO, Universal Laser Systems, Japan) of 30 μm focal spot. The machine was first calibrated to determine the equivalent depth in PMMA material. The calibration was realized one time, per each used lens. PMMA sheets (Spiroplastic, Cairo, Egypt) of 2 mm thickness were used to fabricate the microfluidic chip. For patterning on PMMA sheets, the laser beam with 1000 pulses per inch (PPI) were adjusted to ensure the high-quality of patterning. Also, the laser power was adjusted to 60 % with a speed of 80 % to get optimal dimensions. The chip consisted of 2 PMMA layers: the inlet and outlet were drilled in the top layer, whereas the channels were engraved in the bottom layer. The two layers were adjusted and bonded thermally in a natural ventilation lab oven (STF-N 80, FALC Instruments, Treviglio, Italy) for 13 min at 150 °C while applying a force of 2 N. Afterwards, 1.8 mm outer diameter connection tubes (ULTRAMED, Assiut, Egypt) were attached at


**Fig. 2.** (a) Schematic of the layout of top and bottom layers of the microfluidic chip, and (b) an example of the manufactured chip.

the inlet and outlet holes. The outer diameter of the tube is 1.8 mm, and the inlet and outlet holes are 2 mm, so a small PMMA cylinder with an outer diameter of 2 mm and an inlet diameter of 1.8 mm was added to connect the tubes with the holes avoiding leakage situations. Fig. 2 illustrates the fabricated chip for oocyte denudation.

After fabricating the bottom and top layers, a fluorescent trinocular compound microscope (AmScope FMSYG580TA Supplies 40x-1600x Infinity Plan EPI) was used to measure the channel dimensions such as width and depth of the machined surface. We repeated the measurement technique after chip bonding to ensure the dimensions' low variability. Afterwards, deionized (DI) water was pumped into the chip from the inlet for leakage testing, before moving the oocytes to TCM 199 media to avoid sample loss.

To study the thermal effect of bonding temperature and force, the chip was subjected to 150 °C, in which the set temperature was lower than the melting temperature of PMMA for 13 min, with a bonding force

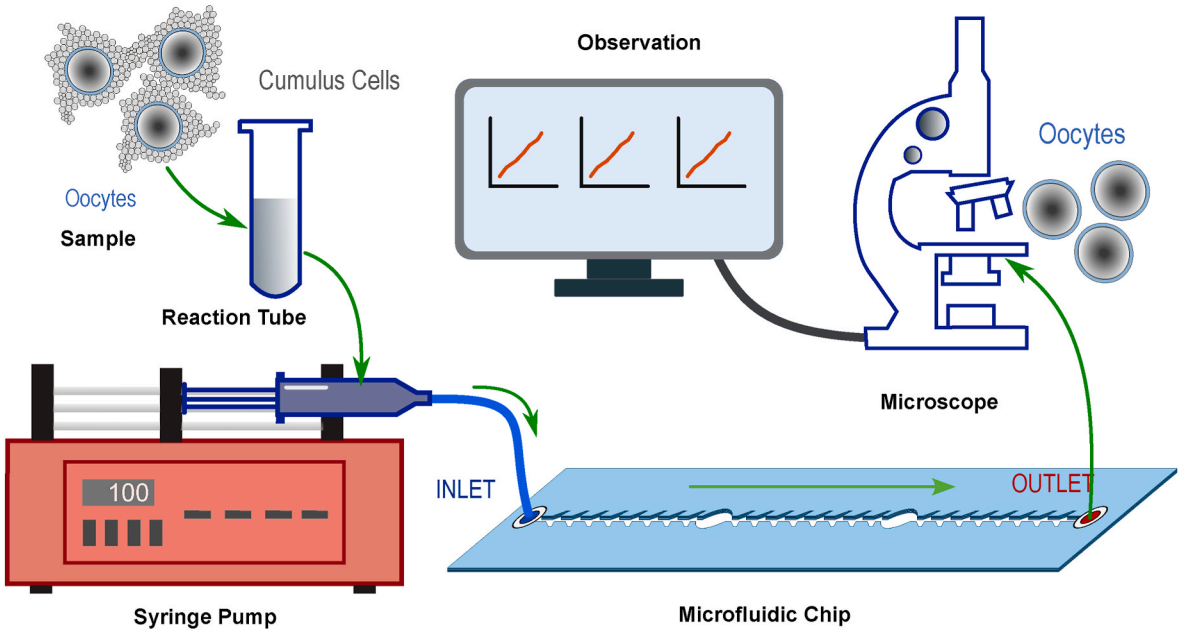


**Fig. 3.** Overall setup for oocyte denudation.

higher than 2 N. Air bubbles and leakage near the holes were observed between the two PMMA layers when applying a force lower than 2 N.

To evaluate the potential of leakages at major junctures, we evaluated the leakage of the chip by increasing the flow rate of the syringe pump to 8 ml/min, and the inlet tube was released from the syringe output port. One of the main benefits of using PMMA for microfluidic systems rather than PDMS is the application of high working flow rates without leakage.

The choice of PMMA over other materials like PDMS is because PMMA is significantly cheaper than PDMS, making it a more cost-effective option for large-scale production. PMMA is more straightforward to fabricate than PDMS, which requires labor-intensive soft lithography; PMMA can be processed using cost-effective methods like CNC milling and laser cutting, reducing manufacturing costs for commercial applications. PMMA is a stiff thermoplastic with more mechanical strength and stability than PDMS, which is flexible and elastic. This rigidity guarantees that microchannel diameters remain constant, decreasing fluid dynamics variability. PMMA chips can be sealed through thermal or solvent bonding methods without requiring plasma treatment.

### 2.4. The effect of wall shear stress

One of the most important aspects in the performance of the proposed microfluidic chip is the wall shear stress that cumulus oocyte cells experience when subjected to jagged units. As such, the wall shear stress is responsible for stripping cumulus corona cell mass. The shear stress is correlated with the flow rate; thus the flow rate must be large enough to strip the cumulus corona cell mass without damaging of oocytes. Calculating the shear stress in cell structures with flow can be realized in multiple ways. Shear stress can be evaluated theoretically or numerically using fluid dynamics. The fluid model of the proposed device is based on the steady-state Naiver–Stokes equation for Newtonian fluid[48]:

$$\frac{\partial u}{\partial t} + (u \cdot \nabla)u - \frac{\mu}{\rho}\nabla^2 u = -\frac{1}{\rho}\nabla p + g \tag{1}$$

where $u$ is the normalized flow velocity vector, $p$ is the pressure, $t$ is the time, $\rho$ is the fluid's density, $\nabla$ is the divergence, $\mu$ is the dynamic viscosity, and $g$ is the gravitational constant. In microfluidic systems, surface forces dominate over volume forces such as gravity.[49] Thus, gravitational force can be neglected. Furthermore, the fluid is assumed to be incompressible, eliminating velocity gradients within the fluid volume.[50] With these assumptions, equation (1) can be simplified to

$$\frac{\partial u}{\partial t} - \frac{\mu}{\rho}\nabla^2 u = -\frac{1}{\rho}\nabla p \tag{2}$$

To calculate the velocity flow, the Navier-Stokes equation must be solved either numerically or analytically to find the velocity profile for the considered geometry. An analytical solution for velocity profiles in rectangular-based microfluidic channels (width ≥ height) was found by expanding the Navier-Stokes equation using the Fourier series.[51]

However, in simple geometry, such as a wide rectangular channel or a tubular channel, computational fluid dynamics was utilized to determine the wall shear stress as a function of the channel width, height, and flow rate. Since the channel length was significantly larger than the channel height, the system can be modeled as a 2D simulation. The wall shear stress can be calculated using the following equation[52]:

$$\tau = \frac{6\eta Q}{h^2 w} \tag{3}$$

where $h$ is the channel height, $w$ is the channel width, $Q$ is the flow rate, and $\eta$ is the medium viscosity. The viscosity of the TCM 199 medium is 0.00089 Pa· s (Pascal second). To modify the shear stress, either the flow rate or dimension of the channel are changed.

The flow rate is as follows,

$$Q = A \cdot v \tag{4}$$

where $A$ is the area, and $v$ is the velocity. Although we inject the fluid constantly, the velocity will change inside the microfluidic channel. Therefore, the shear stress is expected to change at each point in the channel.

### 2.5. Simulations based on computational fluid dynamics

The most crucial factor in oocyte denudation and cumulus cell removal by microfluidic chips is the wall shear stress induced in oocytes going through microfluidic channels. To study the wall shear stress at each point in the microfluidic channels, it is essential to use CFD simulation with a small element size. Also, it is essential to evaluate the shear stress profiles for both distinct inclination angles of the teeth $\theta$ and

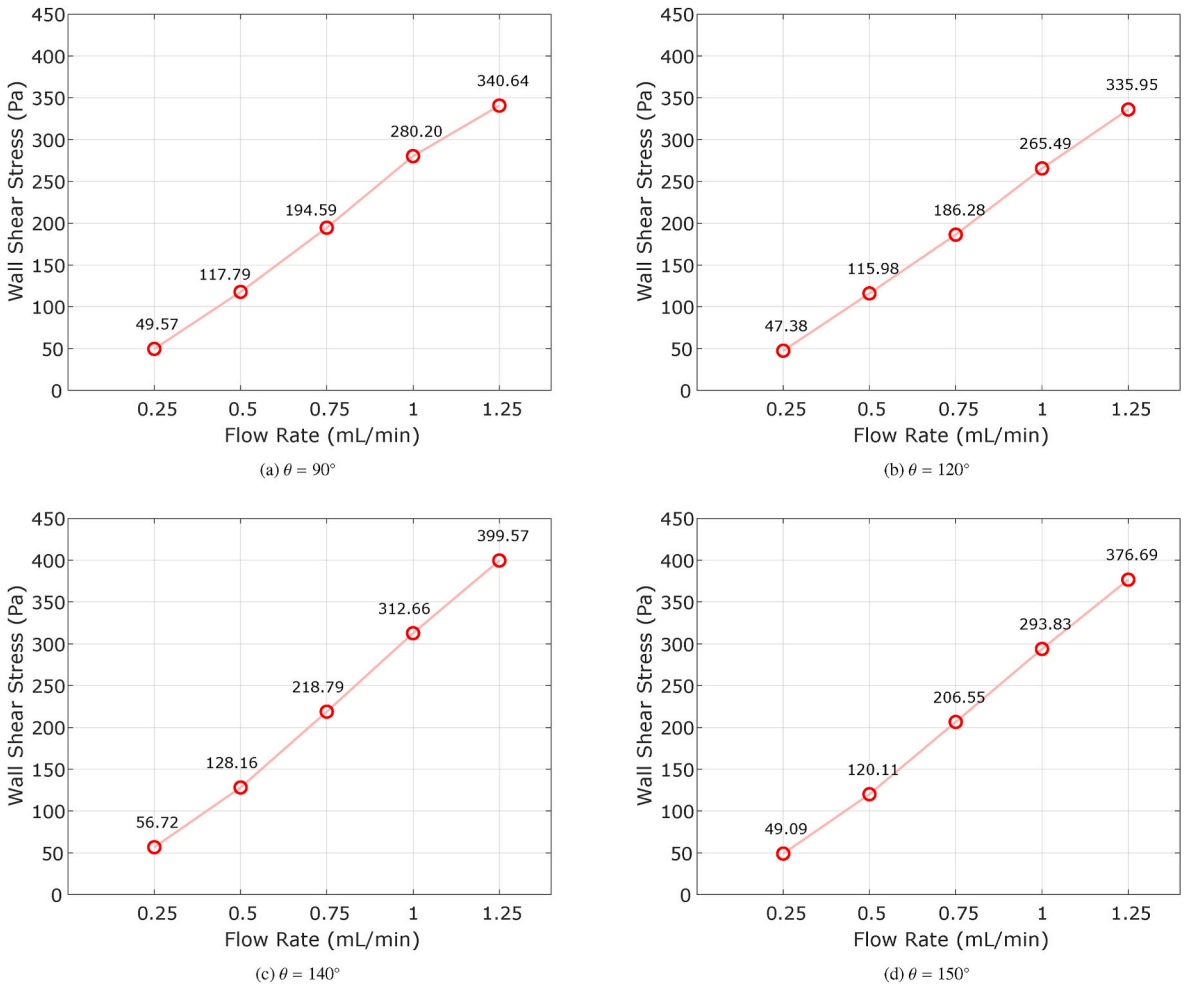


**Fig. 4.** Wall shear stress as a function of flow rate $Q$ and teeth inclination angle $\theta$.

flow rate $Q$. Since the most effective point of the microfluidic channel is located at the beginning of each pair of teeth, higher wall shear stress is expected to be induced on the oocyte at such point, implying the higher likelihood of removing the cumulus corona cells sequentially. Thus, to enable the systematic evaluations considering the above-mentioned points, a three-dimensional (3D) model of the microfluidic chip was conducted on Ansys Fluent 2020 R2 (ANSYS, Inc., Canonsburg, PA) to evaluate and calculate the wall shear stress across the microfluidic channels. The geometry of the microfluidic chip was constructed in Ansys Fluent. Then, the design was extruded with 0.1 mm depth. The overall structure of the design consists of three jagged surface units (each containing 50 teeth) and two expansion units to observe the changes of shear stress in each section.

The inclination angles $\theta = \{90°, 120°, 140°, 150°\}$ were evaluated using both Computational Fluid Dynamics (CFD) simulations and PMMA-based manufactured microfluidic chips. For each of the above-mentioned inclination angle $\theta$, distinct configurations of constant flow rate were applied considering the inlet area of 0.1 mm in width and 0.1 mm in depth.

In the mesh analysis, a named selection was created to specify the inlet, outlet, fluid domain, and wall. Then, the relevant geometry and material were selected. In body sizing, the element size was set at 10 μm, decided after iterative decrements until no variability of output was observed in simulation. As such, the overall geometry resulted in a mesh of over 2.9 million elements and 3.2 million nodes. The setup and solution section used a laminar flow with specified fluid parameters in which the viscosity of the TCM medium was 0.00089 Pa· s. To evaluate the wall shear stress profiles in a plethora of locations along the microchannel, we used 500 contours drawn in the respective walls.

### 2.6. Experimental denudation process

Fig. 3 shows the overall setup involving the oocyte denudation process. After oocyte preparation, 0.75 ml of TCM 199 medium, involving about 9–15 oocytes, was inserted into reaction tubes (Greiner Bio-One Gmbh, Frickenhausen, Germany). A micropipette that fluctuates the 0.75 ml medium is crucial to prevent oocytes from sticking on the tube's wall or bottom. To avoid situations in which the fluid sticks in the tube and does not proceed into the microfluidic chip, we connected the output tube to the 10 ml sterile syringe (Jiangxi Hongda Medical Equipment Group, Nanchang, China), the last of which was fixed on the Syringe Pump (NE-4000, New Era Systems, Grant, FL, USA) and inserted the input tube into the 0.75 ml Micro Centrifuge Tubes. Afterwards, adjust the flow rate and select the proper syringe from the pump's syringe list. Finally, the withdrawal operation is started to pull up the fluid from the reaction tube, pass the designed channel, and store the fluid in the syringe. The above-mentioned procedure has two benefits. First, the fluid can be injected through the channel while avoiding removal of the input tube to infuse air. Second, the injected fluid can be stored in the syringe containing the TCM 199 medium with the denudated oocytes.

Observations of denudated oocytes is realized through camera observations (MT5000 IFR 5.0 MP CCD Sony ICX282AQ sensor), mounted on the Fluorescent Trinocular Compound Microscope (AmScope FMSYG580TA Supplies 40x-1600x Infinity Plan EPI). The microscope

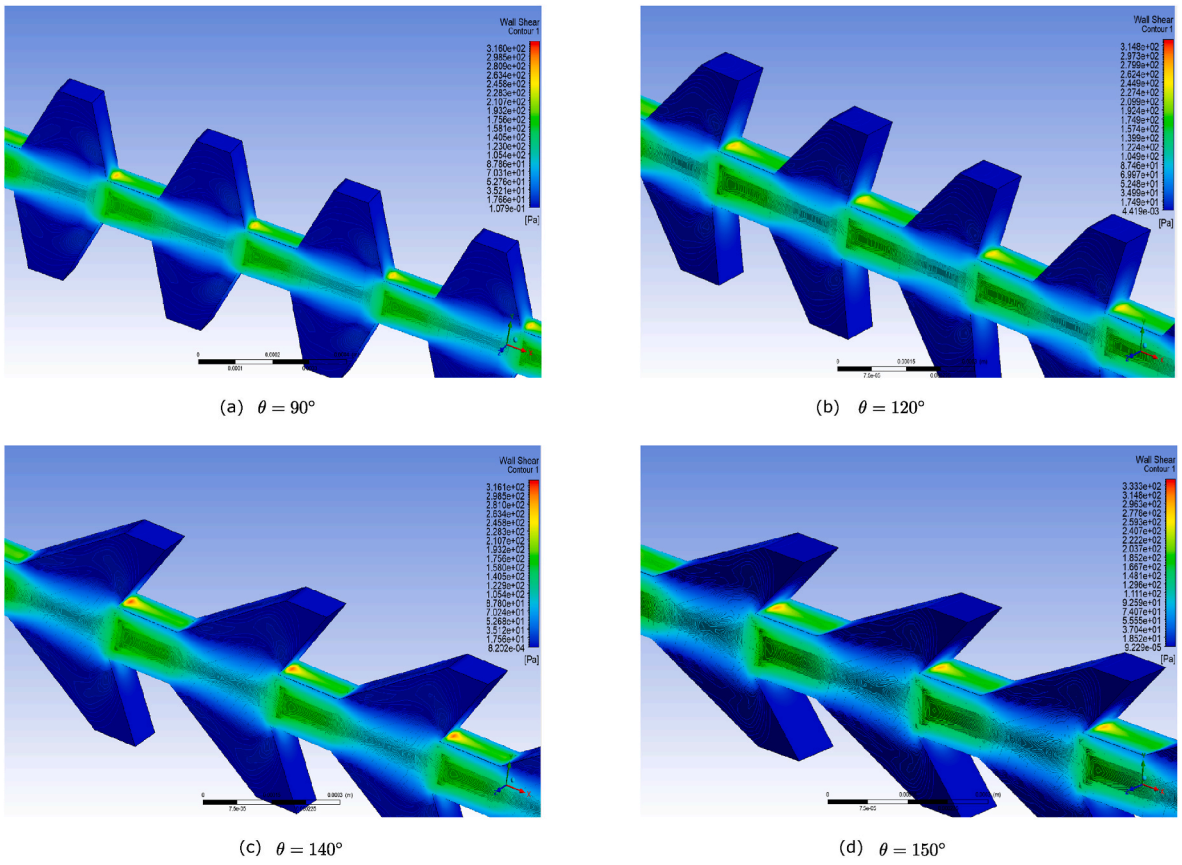


**Fig. 5.** CFD simulation of wall shear stress at 1 ml/min flow rates.

and the camera are connected to a laptop computer for further data analysis. The microfluidic chip is placed on the microscope and connected to the syringe pump, which is to be used at a constant flow rate.

## 3. Results

### 3.1. Computational fluid dynamics (CFD) simulation

In order to show the wall shear stress profiles for distinct configurations of flow rate $Q$ and teeth inclination angle $\theta$. Fig. 4 shows the shear stress profiles for flow rates $Q = \{0.25, 0.5, 0.75, 1, 1.25\}$ ml/min and inclination angles $\theta = \{90°, 120°, 140°, 150°\}$. By observing the results at Fig. 4, we note that higher wall shear stress is achieved at $\theta = 140°$, followed by 150°, 90°, and finally 120°. Due to achieving a high shear stress on the COCs, the most desirable flow rate is observed at 1 ml/min.

In order to render a glimpse of the shear stress across the microfluidic channel, Fig. 5 describes the wall shear stress in detail at a constant flow rate of 1 ml/min on the first pair of teeth. At 1 ml/min flow rate, the maximum wall shear stress at 90° teeth angle is 280.2 Pa, at 120° teeth angle is 265.49 Pa, at 140° teeth angle is 312.66 Pa, and at 150° teeth angle is 293.83 Pa. By observing the results at Fig. 5 and considering the above-mentioned observations of shear stress as a function of flow rate, the inclination angle 140° renders the most desirable profile for

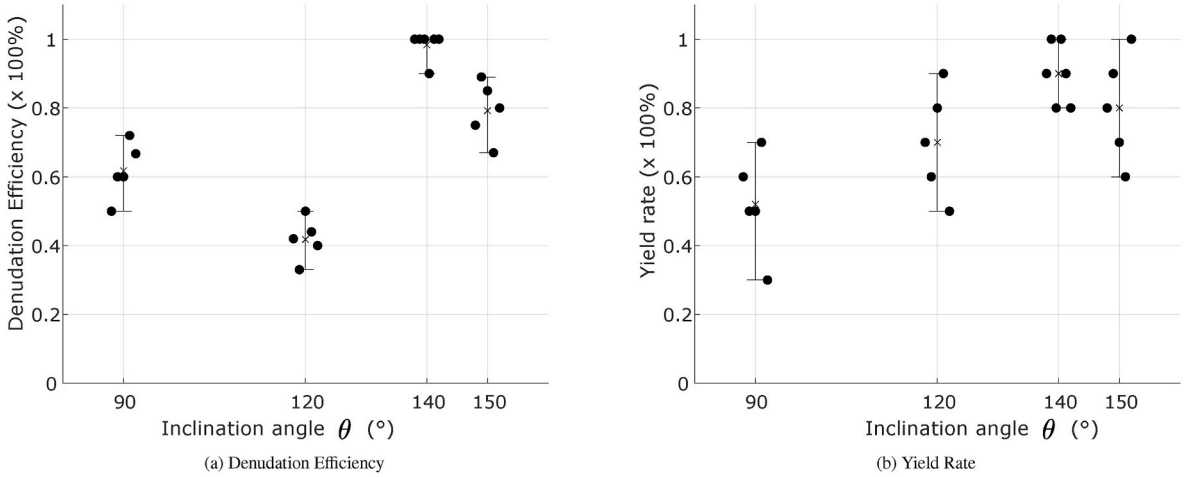


**Fig. 6.** (a) The denudation efficiency and (b) the yield rate as a function of inclination angle $\theta$.

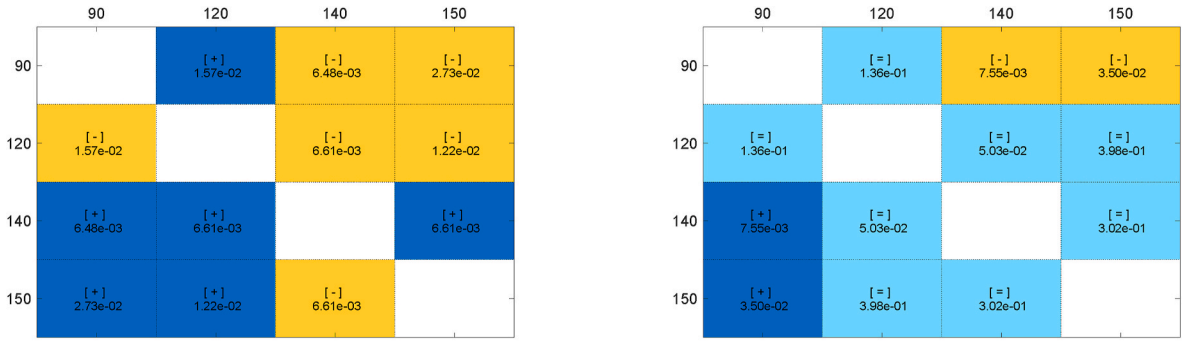


(a) Denudation Efficiency (b) Yield Rate

**Fig. 7.** Statistical comparisons of (a) the denudation efficiency and (b) the yield rate as a function of inclination angle $\theta$.

denudation.

### 3.2. Experimental results

In order to show the denudation performance of the microfluidic chip, we consider the denudation efficiency and yield rate as key performance metrics. Denudation efficiency is the fraction of fully denudated oocytes obtained in the outlet of the chip with respect to the number of output oocytes in the outlet. Yield rate is the percentage of fully or partially denudated oocytes obtained in the output reservoir with respect to the number of oocytes in the inlet.

In order to evaluate the performance under distinct geometry configurations, we manufactured microfluidic chips under distinct configurations of inclination angle $\theta$, specifically 90°, 120°, 140°, and 150°. Also, for simplicity and without loss of generality, we used three jagged surface units (50 teeth at each of them) and two expansion units. Dimensions of the microfluidic chip involve $l_1 = 0.28$ mm, $l_2 = 0.10$ mm, $l_3 = 0.17$ mm, $l_4 = 0.15$ mm, $l_5 = 0.10$ mm, $l_6 = 0.98$ mm, and $l_7 = 0.50$ mm. Furthermore, the microfluidic chip has one inlet and one outlet with a constant depth and width of 0.1 mm. The diameter of the inlet and outlet is 2 mm, and the overall length of the channel of the microfluidic chip is 62.76 mm. For denudation experiments, following the above-mentioned notions on the desirability of the flow rate, we used the constant flow rate of 1 ml/min.

In order to show the oocyte denudation performance of the manufactured microfluid chips, Fig. 6 shows (a) the denudation efficiency and (b) the yield rate for distinct configurations of inclination angles $\theta$. By observing the results of Fig. 6, the reader may note that the maximum denudation efficiency is 96.7 % at $\theta = 140°$, followed by 79.25 % at $\theta = 150°$, 61.62 % at $\theta = 90°$, whereas the minimum efficiency is 42.13 % at $\theta = 120°$. In addition, the maximum yield rate was 90 % at $\theta = 140°$, followed by 80 % at $\theta = 150°$, 70 % at $\theta = 120°$. Furthermore, the observed minimum yield rate is 52 % at $\theta = 90°$.

The sample size is 10 oocytes for each group. In order to show the statistical tests, Fig. 7 shows the Wilcoxon tests at 5 % significance level of (a) the denudation efficiency and (b) the yield rate for distinct configurations of inclination angles $\theta$. The efficiencies and yield rates are compared for statistical significance. Cells with +,-, = indicate when an angle in the row of the cell significantly outperforms, underperforms, and equally performs an angle in the column of the cell. Numbers inside the cell indicate the p-values (smaller values are the better). By looking at the statistical results, one can find that 140° significantly outperforms other inclination angles in terms of denudation efficiency, whereas 140° either outperforms or equally performs compared to other inclination angles. By observing at Fig. 7-(a), one can observe that the configuration angle at 120° outperforms other configurations in terms of denudation efficiency, and the configuration angle at 140° or 150° outperforms other configurations in terms of yield rate.

In order to show a glimpse of the oocyte denudation characteristics rendered by the manufactured microfluid chips, Fig. 8 shows an example of a set of oocytes with cumulus cells subjected to the inlet of the microfluidic chip (state before denudation), and an example of oocytes extracted from the outlet of the microfluidic chip (state after denudation).

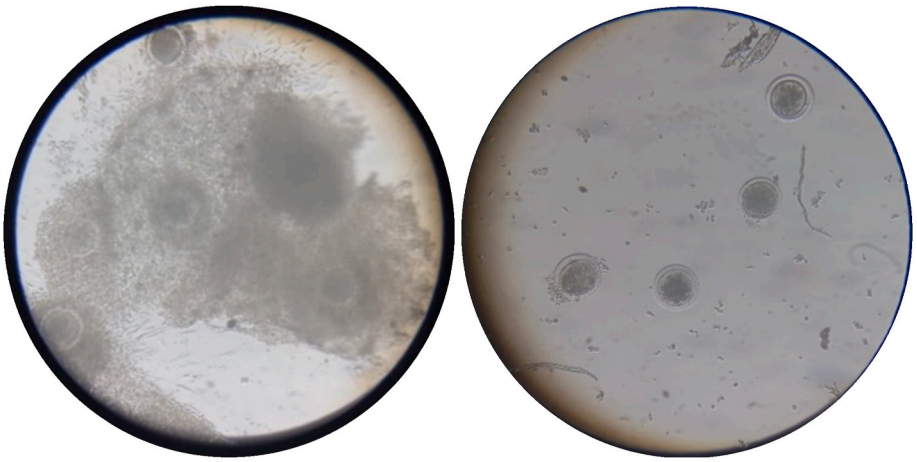

(a) Example of oocytes before denudation (b) Example of oocytes after denudation

**Fig. 8.** (a) Example of a sample of oocyte and cumulus cells, and (b) example of oocytes after denudation process by the proposed microfluidic chip.

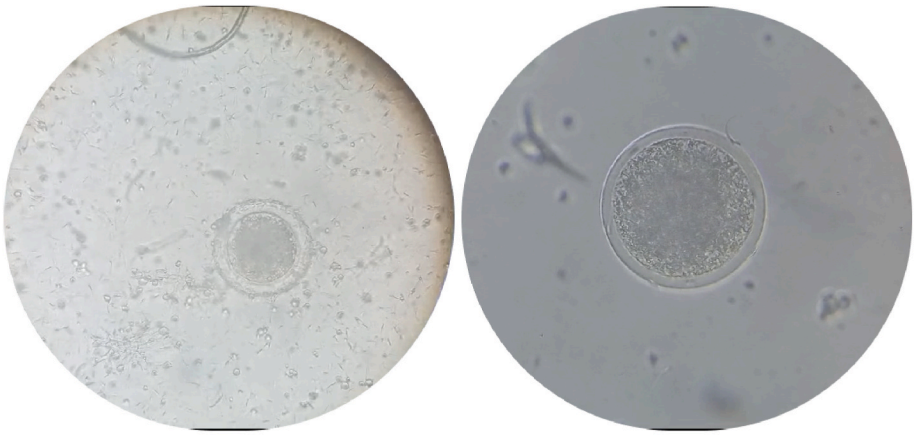


**Fig. 9.** Fertilization process. (a) and (b) the denuded oocyte with qualified sperms.

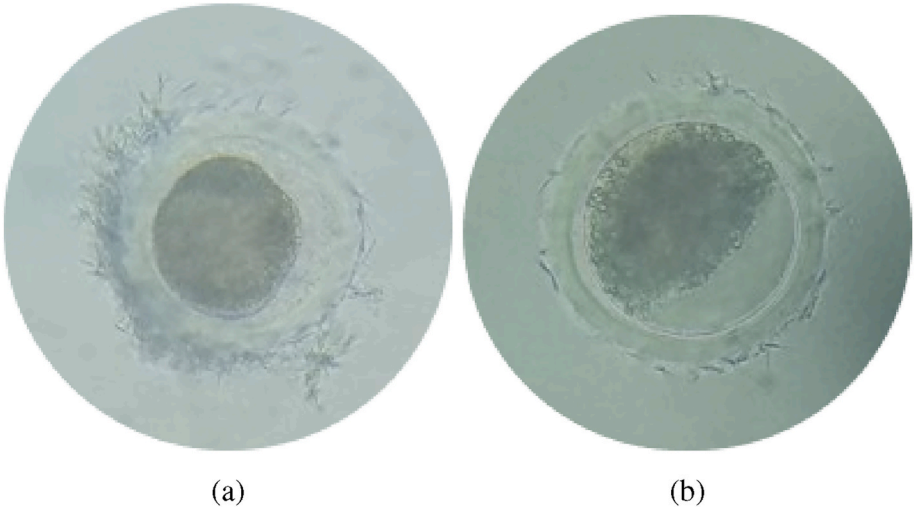


**Fig. 10.** Advanced Fertilization process. (a) morula stage and (b) early blastocyst.

By observing the results in Fig. 8, the reader may note the noticeable differences between inlet and outlet conditions, showing the potential for removal of cumulus cells being adjacent to the oocyte. As for size of oocytes, the oocytes from healthy ovaries of a buffalo have a mean diameter of 146.4 μm,[53] and the oocyte size with the surrounding cumulus cells ranges in the interval 350–450 μm.

It's crucial to guarantee that on-chip denudation doesn't harm the oocytes' fertility and development potential. As a result, we have studied the fertilization rate and embryo development to blastocyst on the denuded oocytes rendered by our microfluidic chip. The fertilization rate represents the percentage of surviving oocytes that progress to two-cell embryos, whereas the blastocyst rate indicates the percentage of two-cell embryos that develop into blastocysts. The average fertilization rate and blastocyst rate of oocytes denuded by the microfluidic chip for IVF were 75.34 % and 94.85 %, respectively. As a result, we observed no adverse effects with respect to post-denudation viability in the long term. Fig. 9 shows the denudated oocytes and qualified sperms were placed in a Petri dish. Supplementary videos illustrating the fertilization process have been included in the supplementary materials section for further reference. Fig. 10 represents the results of the IVF fertilization process, in which the morula and early blastocyst phases have appeared.

## 4. Discussion

The findings show a strong correlation between the inclination angle of the structures of teeth and the efficiency of oocyte denudation. The combination of computational and experimental studies reveals that an inclination angle of 140° achieves the best compromise between exerting enough shear stress for successful cumulus cell elimination and minimizing potential mechanical damage to the oocyte. The CFD models show that this inclination angle produces immense shear stress, which is consistent with experimental data showing the highest denudation efficiency and yield rate. The efficiency variations across inclination angles indicate that optimizing fluid dynamics within the microfluidic chip is crucial for enhancing the denudation process. Furthermore, the reported denudation efficiency of 96.7 % and yield rate of 90 % at 140° demonstrate the system's usefulness in reproductive technologies. This study emphasizes the need for precise microfluidic design in improving ART applications, laying the framework for future modifications and clinical validations.

## 5. Conclusion

In this paper, we proposed a microfluidic chip for oocyte denudation whose structure consists of microchannels hybridizing inner jagged surface and expansion units. The role of the jagged surface units enables

to capitalize from the wall shear stress that act on the cumulus-oocyte-complex to remove the cumulus cells surrounding the oocyte, whereas the (rounded) expansion units facilitate the rotational motions for further deployment to jagged surfaces. The overall structure of the microfluidic chip was manufactured at a low cost profile, benefiting from the features of the engraving technique of a $CO_2$ laser machine on PMMA material. Also, the hybrid between jagged surfaces and expansion units in the channel structure of the chip offers a simple microfluidic device configuration being advantageous to realize the oocyte denudation that circumvents the use of enzymatic components such as hyaluronidase. Computational experiments (ANSYS Fluent 2020 R2) using distinct configurations of the inclination angle of the jagged surfaces and flow rate actuation has allowed to characterize the suitable flow rates for maximal shear stress. Furthermore, the manufactured microfluidic devices has allowed to characterize the denudation performance of 96.7 % and yield rate of 90 % at a constant flow rate of 1 ml/min.

In future work, the effect of the number of expansion units and the number of jagged surface units at the same and different lengths of the channel will be investigated. In addition, we aim to evaluate the quality of oocyte denudation by fertilization process based on IVF techniques.

## CRediT authorship contribution statement

**Ashraf Hisham Dessouky:** Writing – original draft, Software, Methodology, Formal analysis, Data curation, Conceptualization. **Haitham El-Hussieny:** Supervision, Resources, Investigation. **Taymour Mohammed El-Sherry:** Validation, Supervision, Resources, Methodology, Conceptualization. **Victor Parque:** Writing – review & editing, Visualization, Supervision, Software, Data curation. **Ahmed M.R. Fath El-Bab:** Visualization, Validation, Supervision, Methodology, Investigation, Conceptualization.

## Declaration of competing interest

The authors declare that they have no known competing financial interests or personal relationships that could have appeared to influence the work reported in this paper.

## Acknowledgment

The first author is supported by a scholarship from the Egyptian Ministry of Higher Education (MoHE), which is gratefully acknowledged. We thank the Science and Technology Development Fund project (STDF- 12417 and STDF- 46702) and the Japan International Cooperation Agency (JICA) for the use of equipment from the Micro Fabrication Center of E-JUST for this research. Also, we would like to express our deepest gratitude for the elegant effort done by Mr. Sabry Mofty Sabra, Demonstrator, Department of Theriogenology, Faculty of Veterinary Medicine, Assiut University, and Eng. Shimaa El-Sayed, MEMS Lab engineer, Egypt-Japan University of Science and Technology.

## Appendix A. Supplementary data

Supplementary data to this article can be found online at https://doi.org/10.1016/j.biotno.2025.03.001.

## References

1. Zegers-Hochschild F, Adamson GD, Dyer S, et al. The international glossary on infertility and fertility care, 2017. *Fertil Steril*. 2017;108:393–406. https://doi.org/10.1016/j.fertnstert.2017.06.005.
2. Cox CM, Thoma ME, Tchangalova N, et al. Infertility prevalence and the methods of estimation from 1990 to 2021: a systematic review and meta-analysis. *Human Reproduction Open*. 2022;2022:hoac051. https://doi.org/10.1093/hropen/hoac051.
3. W. H. Organization, Infertility Prevalence Estimates 1990-2021, Human Reproduction Open, Licence: CC BY-NC-SA 3.0 IGO 2023 (????).
4. Chambers GM, Sullivan EA, Ishihara O, Chapman MG, Adamson GD. The economic impact of assisted reproductive technology: a review of selected developed countries. *Fertil Steril*. 2009;91:2281–2294. https://doi.org/10.1016/j.fertnstert.2009.04.029.
5. Chian R-C, Lim J-H, Tan S-L. State of the art in in-vitro oocyte maturation. *Curr Opin Obstet Gynecol*. 2004;16.
6. Nosrati R, Graham PJ, Zhang B, et al. Microfluidics for sperm analysis and selection. *Nat Rev Urol*. 2017;14:707–730. https://doi.org/10.1038/nrurol.2017.175.
7. Kashaninejad N, Shiddiky MJA, Nguyen N-T. Advances in microfluidics-based assisted reproductive technology: from sperm sorter to reproductive system-on-a-chip. *Adv Biosyst*. 2018;2, 1700197. https://doi.org/10.1002/adbi.201700197.
8. Sackmann EK, Fulton AL, Beebe DJ. The present and future role of microfluidics in biomedical research. *Nature*. 2014;507:181–189. https://doi.org/10.1038/nature13118.
9. Kashaninejad N, Shiddiky MJA, Nguyen N-T. Advances in microfluidics-based assisted reproductive technology: from sperm sorter to reproductive system-on-a-chip. *Adv Biosyst*. 2018;2, 1700197. https://doi.org/10.1002/adbi.201700197.
10. Whitesides GM. The origins and the future of microfluidics. *Nature*. 2006;442:368–373. https://doi.org/10.1038/nature05058.
11. Clark SG, Haubert K, Beebe DJ, Ferguson CE, Wheeler MB. Reduction of polyspermic penetration using biomimetic microfluidic technology during in vitro fertilization. *Lab Chip*. 2005;5:1229–1232. https://doi.org/10.1039/B504397M.
12. Suh RS, Zhu X, Phadke N, Ohl DA, Takayama S, Smith GD. Ivf within microfluidic channels requires lower total numbers and lower concentrations of sperm. *Hum Reprod*. 2005;21:477–483. https://doi.org/10.1093/humrep/dei323.
13. Han C, Zhang Q, Ma R, et al. Integration of single oocyte trapping, in vitrofertilization and embryo culture in a microwell-structured microfluidic device. *Lab Chip*. 2010;10:2848–2854. https://doi.org/10.1039/C005296E.
14. Rienzi L, Balaban B, Ebner T, Mandelbaum J. The oocyte. *Hum Reprod*. 2012;27:i2–i21. https://doi.org/10.1093/humrep/des200.
15. Mastroianni L, Biggers JD. *Fertilization and Embryonic Development in Vitro*. Plenum Press; 1981. https://doi.org/10.1007/978-1-4684-4016-4.
16. Smith GD, Takayama S. Application of microfluidic technologies to human assisted reproduction. *Mol Hum Reprod*. 2017;23:257–268. https://doi.org/10.1093/molehr/gaw076.
17. Zeringue HC, Beebe DJ, Wheeler MB. Removal of cumulus from mammalian zygotes using microfluidic techniques. *Biomed Microdevices*. 2001;3:219–224. https://doi.org/10.1023/A:1011463330597.
18. Weng L, Lee GY, Liu J, Kapur R, Toth TL, Toner M. On-chip oocyte denudation from cumulus–oocyte complexes for assisted reproductive therapy. *Lab Chip*. 2018;18:3892–3902. https://doi.org/10.1039/C8LC01075G.
19. Zhai R, Shan G, Dai C, et al. Automated denudation of oocytes. *Micromachines*. 2022;13. https://doi.org/10.3390/mi13081301.
20. Mokhtare A, Davaji B, Xie P, et al. Non-contact ultrasound oocyte denudation. *Lab Chip*. 2022;22:777–792. https://doi.org/10.1039/D1LC00715G.
21. Zeringue HC, Rutledge JJ, Beebe DJ. Early mammalian embryo development depends on cumulus removal technique. *Lab Chip*. 2005;5:86–90. https://doi.org/10.1039/B316494M.
22. Chang MC. Fertilization of rabbit ova in vitro. *Nature*. 1959;184:466–467. https://doi.org/10.1038/184466a0.
23. A N, M G, K V, R B. Recovery and in vitro culture of preimplantation-stage embryos. In: Nagy A, Gertsenstein M, Vintersten K, Behringer R, eds. *Manipulating the Mouse Embryo*. Cold Spring Harbor Laboratory Press; 2003.
24. Stern R, Jedrzejas MJ. Hyaluronidases: their genomics, structures, and mechanisms of action. *Chem Rev*. 2006;106:818–839. https://doi.org/10.1021/cr050247k, 10.1021/cr050247k.
25. Camaioni A, Hascall V, Yanagishita M, Salustri A. Effects of exogenous hyaluronic acid and serum on matrix organization and stability in the mouse cumulus cell-oocyte complex. *J Biol Chem*. 1993;268:20473–20481. https://doi.org/10.1016/S0021-9258(20)80750-9.
26. Cross PC, Brinster RL. In vitro development of mouse oocytes1. *Biol Reprod*. 1970;3:298–307. https://doi.org/10.1093/biolreprod/3.3.298.
27. Itagaki Y, Toyoda Y. Effects of prolonged sperm preincubation and elevated calcium concentration on fertilization of cumulus-free mouse eggs < i>in vitro</i&gt. *J Reprod Dev*. 1992;38:219–224. https://doi.org/10.1262/jrd.38.219.
28. Evison M, Pretty C, Taylor E, Franklin C. Human recombinant hyaluronidase (cumulase®) improves intracytoplasmic sperm injection survival and fertilization rates. *Reprod Biomed Online*. 2009;18:811–814. https://doi.org/10.1016/S1472-6483(10)60030-2.
29. Taylor TH, Elliott T, Colturato LF, Straub RJ, Mitchell-Leef D, Nagy ZP. Comparison of bovine- and recombinant human-derived hyaluronidase with regard to fertilization rates and embryo morphology in a sibling oocyte model: a prospective, blinded, randomized study. *Fertil Steril*. 2006;85:1544–1546. https://doi.org/10.1016/j.fertnstert.2005.10.053.
30. Lee JH, Yoo M, Lee SM, Park S-J, Kil TY, Kim MK. Toxicity of the recombinant human hyaluronidase alt-bc4 on embryonic development. *J Anim Sci Technol*. 2021;63:272–280. https://doi.org/10.5187/jast.2021.e34.
31. Ishizuka Y, Takeo T, Nakao S, et al. Prolonged exposure to hyaluronidase decreases the fertilization and development rates of fresh and cryopreserved mouse oocytes. *J Reprod Dev*. 2014;60:454–459. https://doi.org/10.1262/jrd.2014-045.
32. Iwasaki W, Yamanaka K, Sugiyama D, et al. Simple separation of good quality bovine oocytes using a microfluidic device. *Sci Rep*. 2018;8, 14273. https://doi.org/10.1038/s41598-018-32687-6.
33. Luo Z, Güven S, Gozen I, et al. Deformation of a single mouse oocyte in a constricted microfluidic channel. *Microfluid Nanofluidics*. 2015;19:883–890. https://doi.org/10.1007/s10404-015-1614-0.

34. Islam MM, Loewen A, Allen PB. Simple, low-cost fabrication of acrylic based droplet microfluidics and its use to generate dna-coated particles. *Sci Rep*. 2018;8:8763. https://doi.org/10.1038/s41598-018-27037-5.
35. Nasser GA, Fath El-Bab AM, Abdel-Mawgood AL, Mohamed H, Saleh AM. Co2 laser fabrication of pmma microfluidic double t-junction device with modified inlet-angle for cost-effective pcr application. *Micromachines*. 2019;10. https://doi.org/10.3390/mi10100678. URL: https://www.mdpi.com/2072-666X/10/10/678.
36. Adel M, Allam A, Sayour AE, Ragai HF, Umezu S, Fath El-Bab AMR. Fabrication of spiral low-cost microchannel with trapezoidal cross section for cell separation using a grayscale approach. *Micromachines*. 2023;14. https://doi.org/10.3390/mi14071340. URL: https://www.mdpi.com/2072-666X/14/7/1340.
37. Mofadel H, Hussien H, Fath El-Bab A, El-Sherry T. Bull sperm rheotaxis and kinematics in microfluidic channels with different heights. *Assiut Vet Med J*. 2024;70:50–61. https://doi.org/10.21608/avmj.2023.228274.1176.
38. Mofadel HA, Hussein HA, Abd-Elhafee HH, El-Sherry TM. Impact of various cryopreservation steps on sperm rheotaxis and sperm kinematics in bull. *Sci Rep*. 2024;14, 11403. https://doi.org/10.1038/s41598-024-61617-y.
39. Mansour H, Soliman EA, El-Bab AMF, Abdel-Mawgood AL. Development of epoxy resin-based microfluidic devices using co2 laser ablation for dna amplification point-of-care (poc) applications. *Int J Adv Des Manuf Technol*. 2022;120:4355–4372. https://doi.org/10.1007/s00170-022-08992-w.
40. Nasser GA, Abdel-Mawgood AL, Abouelsoud AA, Mohamed H, Umezu S, El-Bab AMRF. New cost effective design of pcr heating cycler system using peltier plate without the conventional heating block. *J Mech Sci Technol*. 2021;35:3259–3268. https://doi.org/10.1007/s12206-021-0646-5.
41. Ngum LF, Matsushita Y, El-Mashtoly SF, Fath El-Bab AMR, Abdel-Mawgood AL. Separation of microalgae from bacterial contaminants using spiral microchannel in the presence of a chemoattractant. *Bioresources and Bioprocessing*. 2024;11:36. https://doi.org/10.1186/s40643-024-00746-8.
42. Hashem R, El-Hussieny H, Umezu S, El-Bab AMRF. Soft tissue compliance detection in minimally invasive surgery: dynamic measurement with piezoelectric sensor based on vibration absorber concept. *Journal of Robotics and Control*. 2024;5. https://doi.org/10.18196/jrc.v5i5.22895.
43. Prakash S, Kumar S. Fabrication of microchannels on transparent pmma using co2 laser (10.6 $\mu$m) for microfluidic applications: an experimental investigation. *Int J Precis Eng Manuf*. 2015;16:361–366. https://doi.org/10.1007/s12541-015-0047-8.
44. Helmy M, Fath El-Bab AM, El-Hofy H. Elimination of clogging in pmma microchannels using water assisted co2 laser micromachining. In: *Mechanical and Electrical Technology VII, Volume 799 of Applied Mechanics And Materials*. Trans Tech Publications Ltd; 2015:407–412. https://doi.org/10.4028/www.scientific.net/AMM.799-800.407.
45. Chen X, Li T, Shen J. Co2 laser ablation of microchannel on pmma substrate for effective fabrication of microfluidic chips. *Int Polym Process*. 2016;31:233–238. https://doi.org/10.3139/217.3184.
46. Imran M, Rahman RA, Ahmad M, Akhtar MN, Usman A, Sattar A. Fabrication of microchannels on pmma using a low power co2 laser. *Laser Phys*. 2016;26, 096101. https://doi.org/10.1088/1054-660X/26/9/096101.
47. Prakash S, Kumar S. Fabrication of rectangular cross-sectional microchannels on pmma with a co2 laser and underwater fabricated copper mask. *Opt Laser Technol*. 2017;94:180–192. https://doi.org/10.1016/j.optlastec.2017.03.034.
48. Pelesko JA, Bernstein DH. *Modeling MEMS and NEMS*. CRC Press; 2002. https://doi.org/10.1201/9781420035292.
49. Panigrahi PK. *Transport Phenomena in Microfluidic Systems*. John Wiley & Sons Singapore Pte. Ltd; 2016. https://doi.org/10.1002/9781118298428.
50. Kim TH, Lee JM, Ahrberg CD, Chung BG. Development of the microfluidic device to regulate shear stress gradients. *BioChip Journal*. 2018;12:294–303. https://doi.org/10.1007/s13206-018-2407-9.
51. Bruus H. Acoustofluidics 1: governing equations in microfluidics. *Lab Chip*. 2011;11:3742–3751. https://doi.org/10.1039/C1LC20658C.
52. Rossi M, Lindken R, Hierck BP, Westerweel J. Tapered microfluidic chip for the study of biochemical and mechanical response at subcellular level of endothelial cells to shear flow. *Lab Chip*. 2009;9:1403–1411. https://doi.org/10.1039/B822270N.
53. Raghu HM, Nandi S, Reddy SM. Follicle size and oocyte diameter in relation to developmental competence of buffalo oocytes < emph type=”2”>in vitro</ emph&gt. *Reprod Fertil Dev*. 2002;14:55–61. https://doi.org/10.1071/RD01060.